DOI: 10.4149/BLL_2023_002

Bratisl Med J 2023; 124 (1)

12 – 24

MATHEMATICAL METHODS

Recognizing seizure using Poincaré plot of EEG signals and graphical features in DWT domain

Hesam AKBARI[1], Muhammad Tariq SADIQ[2], Nastaran JAFARI[3], Jingwei TOO[4], Nasser MIKAEILVAND[5], Antonio CICONE[6], Stefano SERRA-CAPIZZANO[7]

Department of Biomedical Engineering, South Tehran Branch, Islamic Azad University, Tehran, Iran.
st_h.akbari@azad.ac.ir

ABSTRACT
Electroencephalography (EEG) signals are considered one of the oldest techniques for detecting disorders in medical signal processing. However, brain complexity and the non-stationary nature of EEG signals represent a challenge when applying this technique. The current paper proposes new geometrical features for classification of seizure (S) and seizure-free (SF) EEG signals with respect to the Poincaré pattern of discrete wavelet transform (DWT) coefficients. DWT decomposes EEG signal to four levels, and thus Poincaré plot is shown for coefficients. Due to patterns of the Poincaré plot, novel geometrical features are computed from EEG signals. The computed features are involved in standard descriptors of 2-D projection (STD), summation of triangle area using consecutive points (STA), as well as summation of shortest distance from each point relative to the 45-degree line (SSHD), and summation of distance from each point relative to the coordinate center (SDTC). The proposed procedure leads to discriminate features between S and SF EEG signals. Thereafter, a binary particle swarm optimization (BPSO) is developed as an appropriate technique for feature selection. Finally, k-nearest neighbor (KNN) and support vector machine (SVM) classifiers are used for classifying features in S and SF groups. By developing the proposed method, we have archived classification accuracy of 99.3 % with respect to the proposed geometrical features. Accordingly, S and SF EEG signals have been classified. Also, Poincaré plot of SF EEG signals has more regular geometrical shapes as compared to S group. As a final remark, we notice that the Poincaré plot of coefficients in S EEG signals has occupied more space as compared to SF EEG signals *(Tab. 3, Fig. 11, Ref. 57)*. Text in PDF *www.elis.sk*
KEY WORDS: EEG signal, DWT, Poincaré plot, geometrical feature, BPSO, SVM, KNN.

Introduction

Abnormal conflicts of the brain may contribute to epilepsy when taken into account as a chronic neurological disorder (1). Nearly 50 million humans suffer from epilepsy, mainly those living in the developing countries (2). Detection of seizures is crucial in the treatment of patients with epilepsy. In most patients with epilepsy, there are no definite clinical signs for seizures. Electroencephalography (EEG) signals are highly utilized in detecting brain activities and disorders such as depression (3, 4), brain-computer interface (BCI) (5–7), schizophrenia (8), alcoholism (9) and sleep apnea (10). Spikes are regularly evident in EEG signals of the human brain for epileptic seizures (11, 12). These phenomena can visually be evaluated via specialists in this field. In long EEG records, the visual inspection can be a cumbrous and time-consuming action aimed at detecting the presence of epileptic seizures (1, 13, 14). Therefore, an automatic method would be required to classify seizure (S) and seizure-free (SF) EEG signals. According to the literature, several methods have been developed for this purpose. Some of the methods are comprised of permutation entropy (15), horizontal visibility graph (HVG) (16), clustering technique (17), linear prediction error energy (18), fractional linear prediction (FLP) error (19), dual-tree complex wavelet transform (DT-CWT) (20), autoregressive modeling (21), tunable-Q wavelet transform (TQWT) (13, 22), reconstructed phase space (RPS) (14), second-order difference plot (SODP) (23, 24) , and improved eigenvalue decomposition of Hankel matrix and Hilbert transform (IEVDHM–HT) (25). Most of the latter methods work on the basis of nonlinear features extraction.

[1]Department of Biomedical Engineering, South Tehran Branch, Islamic Azad University, Tehran, Iran, [2]School of Architecture, Technology and Engineering, University of Brighton, Brighton, United Kingdom, [3]Department of Biomedical Engineering, School of Advanced Medical Technology, Isfahan University of Medical Sciences, Isfahan, Iran, [4]Faculty of Electrical Engineering, Universiti Teknikal Malaysia Melaka, Hang Tuah Jaya, Durian Tunggal, Melaka, Malaysia, [5]Department of Mathematics, Ardabil branch, Islamic Azad University, Ardabil, Iran, [6]Department of Information Engineering, Computer Science and Mathematics, University of L'Aquila, L'Aquila, Italy, and Istituto di Astrofisica e Planetologia Spaziali, INAF, Rome, Italy, and Istituto Nazionale di Geofisica e Vulcanologia, Rome, Italy, and [7]Department of Science and High Technology, Division of Mathematics, University of Insubria, Como, Italy, and Department of Information Technology, Division of Scientific Computing, Uppsala University, Uppsala, Sweden

Address for correspondence: Hesam AKBARI, Department of Biomedical Engineering, South Tehran Branch, Islamic Azad University, Tehran, Iran.

To decompose the input signal into intrinsic mode functions (IMFs), empirical mode decomposition (EMD) has been suggested (26). For the first time, SODP (24) and RPS (27) are utilized to prepare a 2-D representation for IMFs of EEG signals to classify EEG signals in S and SF groups (24, 27), in which the 95 % confident area measure of 2-D representation of IMFs was applied to differentiate features between S and SF EEG signals (24, 27). The achieved results were promising but based on EMD which suffers from the mod-mixing problem. In addition, the results are sensitive to noise.

In the past, two methods, RPS (27) and SODP (24), have been used in representation of the EEG signal in 2-D space. The RPS technique requires two variables to be estimated, namely time delay and embedding dimension (28, 29). These two parameters are computed with respect to mutual information (MI) and false nearest neighbor (FNN) (8, 28), respectively. The drawback of the RPS technique lies in the time-consuming nature of the procedure, particularly because the MI and FNN calculations are highly burdensome. Although SODP, unlike RPS, can illustrate the EEG signals without any parameter calculation, SODP illustrates the variability of the signal, not the signal itself (23, 30). In other words, SODP cannot illustrate the complex nature of the signal (12). The Poincaré plot method can show complex behaviors of the signal without any estimation of parameters, which makes it fast as opposed to the time-consuming procedure employed in the technique of RPS (29, 31). On the other hand, the Poincaré plot illustrates the signal itself, unlike SODP which illustrates the signal variability (1, 31). Nowadays, discrete wavelet transform (DWT) is becoming one of the popular tools in biomedical signal processing applications. The DWT is held to be a suitable method for analyzing the dynamics of non-stationary signals like bio-signals (32) which, unlike EMD, is not sensitive to noise (33), as well as for its intrinsic numerical stability.

Recently, a new group of features called geometrical features have been proposed to evaluate the complex behavior of biomedical signals plotted in 2-D space. In study (34), the phonocardiogram (PCG) has been plotted in 2-D space by RPS, and then the geometrical features were extracted to detect valvular heart diseases. In another research (35), the geometrical features of modes of EEG signals in EMD and variational mode decomposition (VMD) domains have been used to detect alcoholism disorders. These geometrical features also could decode the chaotic behavior of muscle diseases by plotting electromyogram (EMG) signals in a 2-D complex plane (36). In other works (28, 30), the geometrical features of RPS and SODP of EEG signals have been used to detect depressed subjects. Also, the geometrical properties have shown an acceptable performance also in classifying RPS of EEG signals in normal individuals and those suffering from schizophrenia (8). These successes of geometrical features motivate us to apply ideas related to detecting seizures by EEG signals.

By checking the previous works which have been done to detect seizure EEG signals, we can understand that in most of the proposed frameworks, extracted features were fed to classifiers, which makes those methods quite complex; in fact, selecting the

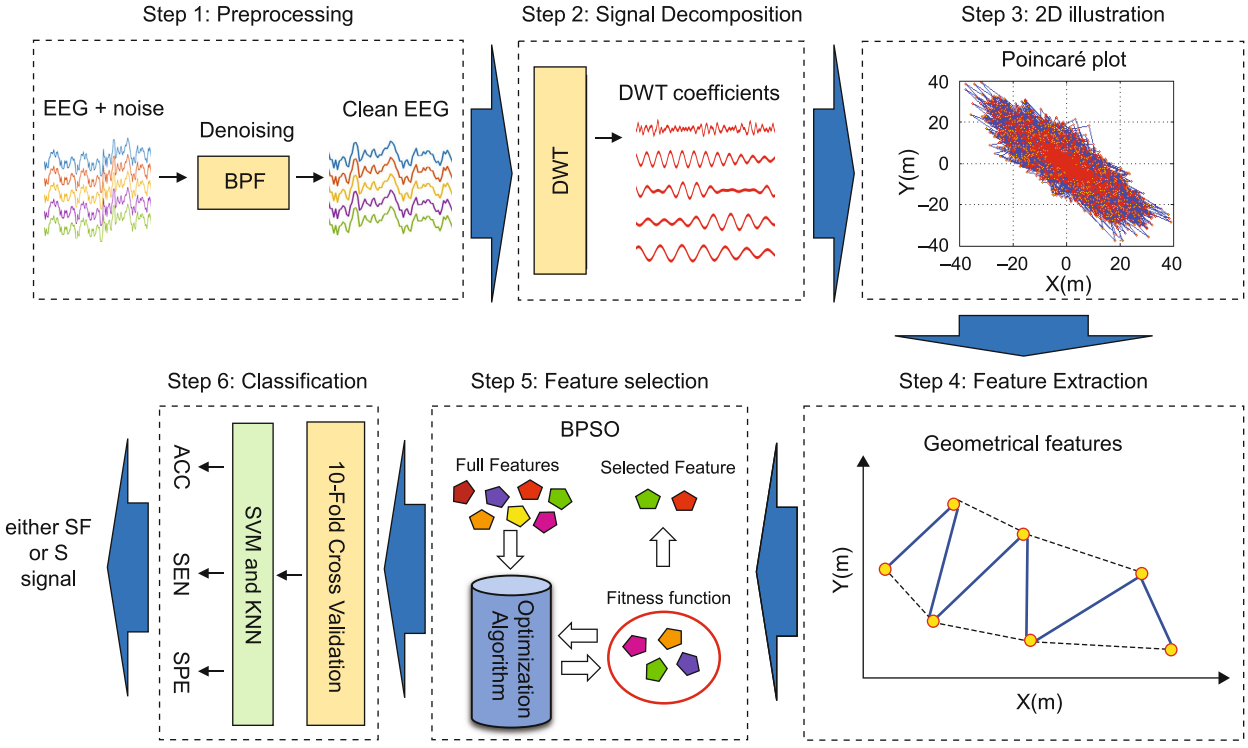

Fig. 1. Proposed method.

best features before classification allows the proposed framework to become faster and simpler. Hence, in this work, binary particle swarm optimization (BPSO) is used to select the best features to increase the performance of the proposed framework and decrease the complexity of classification.

In this paper, the first step is associated with decomposing DWT to EEG signals. The motivation comes from the success of DWT in previous works (37, 38). In the next step, the Poincaré plot is utilized to create a 2-D representation for DWT coefficients. Due to Poincaré plot of coefficients, novel geometrical features are extracted for differentiating S and SF EEG signals. These features are comprised of standard descriptors of 2-D projection (STD), summation of triangle area using consecutive points (STA), as well as summation of the shortest distance from each point relative to the 45-degree line (SSHD), and summation of distance from each point relative to the coordinate center (SDTC). Afterward, BPSO is developed as a feature selection technique. Finally, k-nearest neighbor (KNN) and support vector machine (SVM) classifiers are utilized to classify features in S and SF groups.

The paper is organized as follows:

In Section 2 we present and discuss the proposed techniques, including the used database, DWT, Poincaré plot, as well as BPSO and classifiers. The empirical results are shown in Section 3. The paper discussion of this study is contained in Section 4 and finally, conclusions are drawn in Section 5.

Proposed method

In the current work, the first step is to decompose the input EEG signals by DWT to four levels, which results in five components. Then, in order to decode the behaviors of EEG signals in S and SF groups, the 2-D illustration of coefficients is reconstructed by the Poincaré plot. After that, the geometrical features are quantized by the complex behaviors of Poincaré plot in 2-D space. Finally, the selected features by BPSO are fed to SVM and KNN classifiers to detect S and SF EEG signals. The steps of the proposed framework are shown in Figure 1.

Used database

A benchmark dataset, which can be downloaded for free from the Bonn University website, has been analyzed by employing the method proposed in study (39). Five subsets assigned as A, B, C, D, and E make up this database. Each subset contains 100 EEG signals sampled at 173.61 Hz. Each EEG signal has a duration of 23.6 seconds wherefore 4,097 samples are obtained. Subset A and subset B were recorded from five healthy individuals in two conditions of eyes opened and closed, respectively. Those records from five patients with seizure control who recovered from surgery of epileptic locations are allocated to subsets C and D. Subset E consists of EEG signals with regard to the epileptic seizure activity perceived in the epileptic region. In this work, the signals within subsets C and D are regarded as SF EEG signals, while the signals within subset E are regarded as S EEG signals (C, D vs E). For removing the noise and artifacts, a fourth-order Butterworth band-pass filter with respect to 0.53 to 40 Hz bandwidth has been used to filter EEG signals.

Discrete wavelet transform (DWT)

Discrete wavelet transform (DWT) is considered a prevalent tool in bio-signals applications (40). By applying filter bank, DWT decomposes the input signal into its sub-bands. At the first level of decomposition, DWT is filtered to the input signal by low pass filter (LPF) and high pass filter (HPF) with respect to $[0,\pi/2]$ and $[\pi/2, \pi/4]$ bandwidths, respectively. The output of HPF and LPF are associated with detail 1 (D_1) and approximation 1 (A_1), respectively. At the second level decomposition, A_1 is filtered to

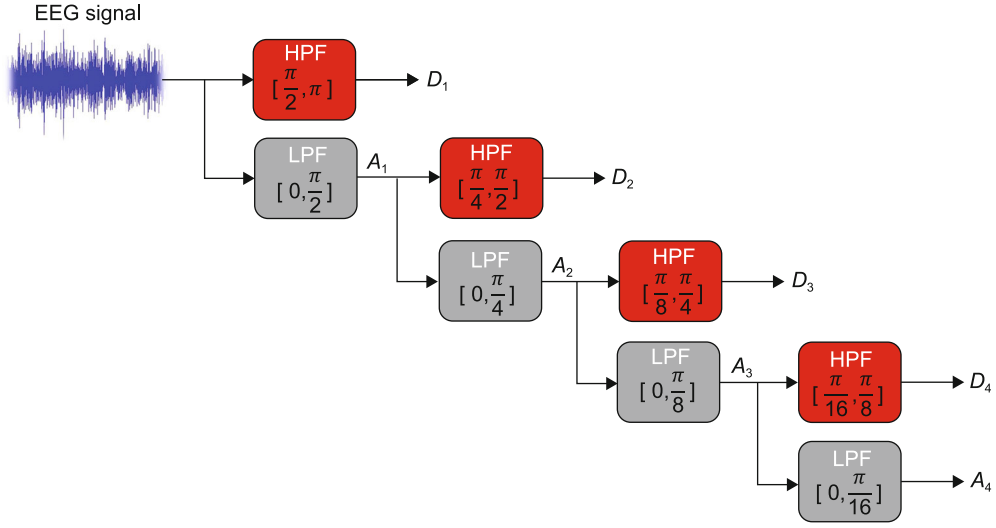

Fig. 2. Block diagram for DWT filter bank in 4-level decomposition.

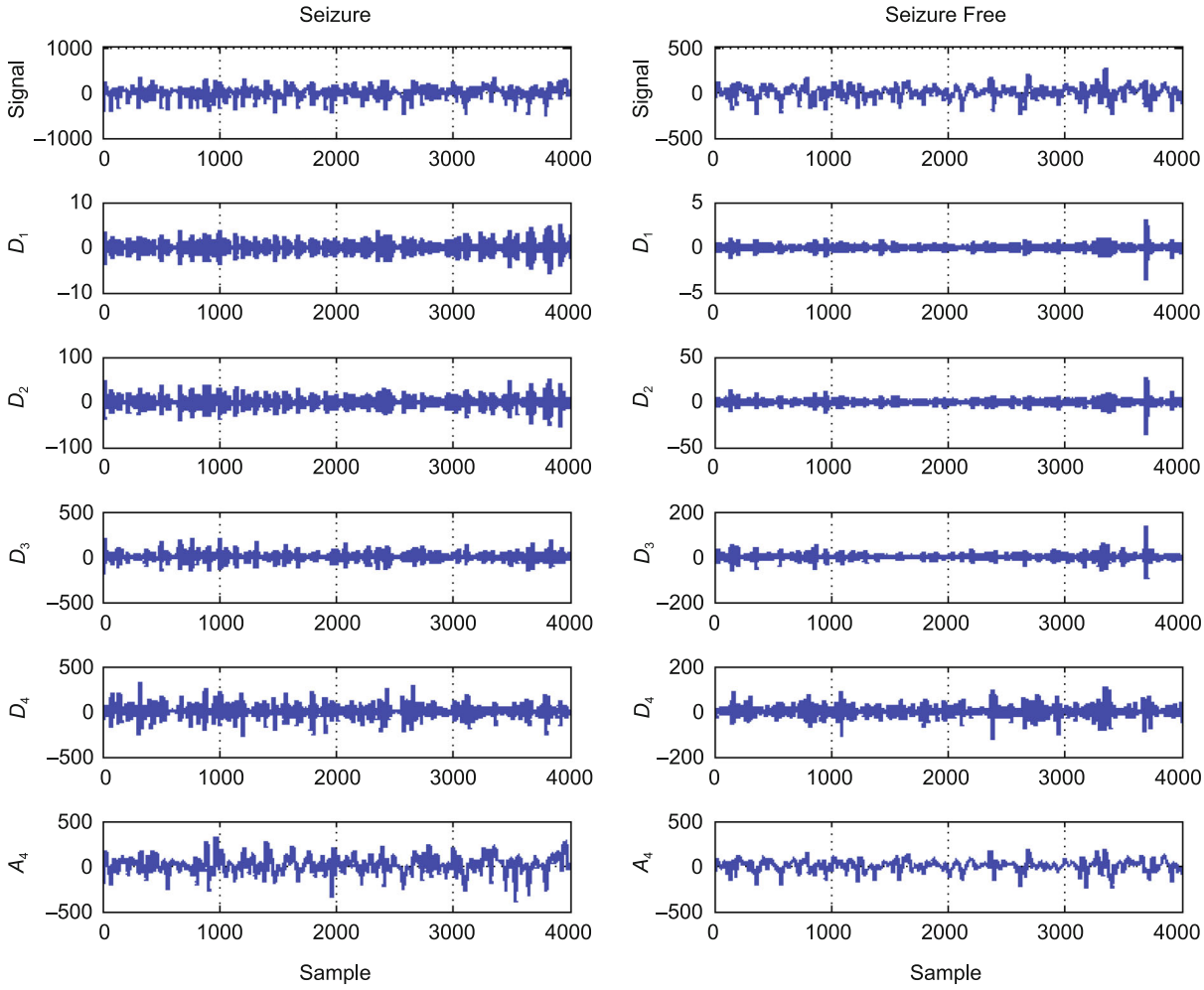

Fig. 3. The plots (from up to down) show a sample of EEG signal and its D_1 , D_2 , D_3 , D_4 and A_4 for S (left) and SF (right) groups.

HPF and LPF with respect to [0,π/4] and [π/4, π/2] bandwidths, leading to obtain A_2 and D_2, respectively. Generally, at the n-th level decomposition (n>1), A_n and D_n are obtained by the filter of A_{n-1} using LPF and HPF with respect to $[0,\pi/2^n]$ and $[\pi/2^n, \pi/2^{n-1}]$ bandwidths, respectively. In other words, at the n-th level of DWT decomposition, n+1 sub-bands result in one approximation and n details (i.e., A_n, D_n, D_{n-1}, … , D_1). By using DWT, many wavelet functions are proposed to decompose the input signal (41). In this work, Daubechies order 4 (db4) wavelet function is used for decomposing EEG signals. Figure 2 shows the block diagram for DWT filters in 4 levels of decomposition. Figure 3 indicates the filtered S and SF EEG signals and its five extracted DWT coefficients.

Poincaré plot

The Poincaré plot is used to show the behavior of signals in a 2-D projection (31, 42). In this paper, the Poincaré plot of coefficients is utilized as a visual image for evaluating the dynamical behavior in S and SF EEG signals.

Let us assume that the EEG input signal is a sequence such as $x(n) = [x_1, x_2, x_3, ..., x_n]$. Then, we define $X(m)$ and $Y(m)$ as follows (43):

$$X(m) = [x_1, x_2, x_3, ..., x_{n-1}], \quad (1)$$

$$Y(m) = [x_2, x_3, x_4, ..., x_n]. \quad (2)$$

Finally, the Poincaré plot represents the complexity of the signal $x(n)$, by plotting X(m) versus Y(m) as follows:

$$[X(m)\ Y(m) = [(x_1, x_2)_1, (x_2, x_3)_2, ..., (x_{n-1}, x_n)_{n-1}]. \quad (3)$$

Figure 4 shows a sample for Poincaré plot of coefficients in S and SF EEG signals. Due to the 2D projection of the pattern of the coefficients, we can compute the significant geometrical features to discriminate between S and SF EEG signals.

Figure 4 reveals that the Poincaré plot of coefficients contains geometrical patterns. In addition, Poincaré plot for DWT coefficient of S EEG signals occupies a larger area than the same Poin-

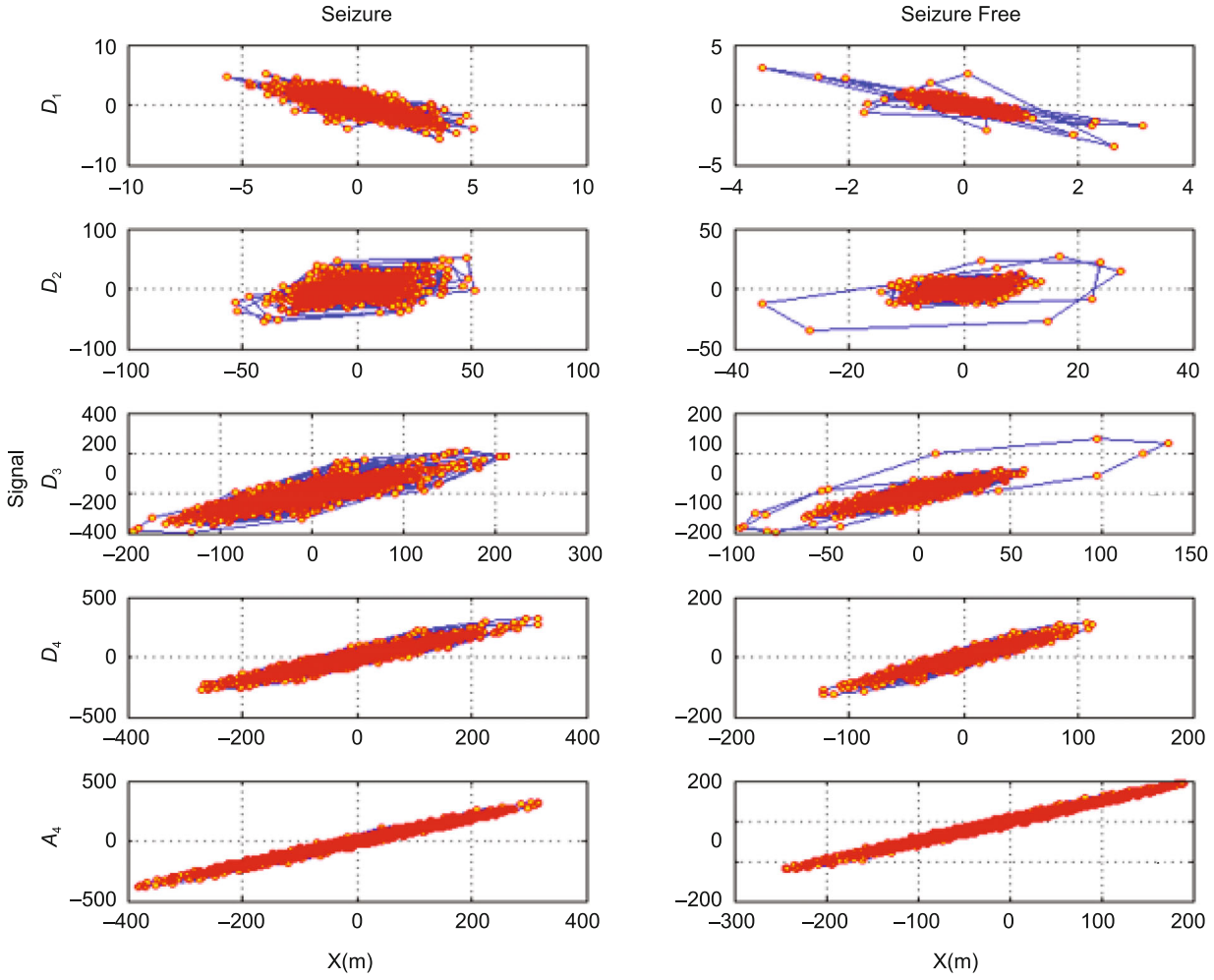

Fig. 4. The plots (from up to down) show the Poincaré plot of D_1 , D_2 , D_3, D_4 and A_4 for a sample of S (left) and SF (right) EEG signals.

caré plot for DWT coefficient of SF EEG signals. It motivates us to compute the geometric features for classification of S and SF EEG signals.

Geometrical features extraction

In this work, new geometrical features are proposed for extracting the geometric pattern from Poincaré plot of coefficients, as described in the following text.

Standard descriptors of 2-D projection (STD)

The scattering of points can be a useful parameter for measuring the value of variation for a 2D shape (43). In order to quantize the scattering of the point in 2-D space, two parameters are defined as follows:

$$SD1 = (\text{Var}\ (d1))^{1/2}, \quad (4)$$
$$SD2 = \text{Var}\ (d2))^{1/2}, \quad (5)$$

where SD1 and SD2 measure the scattering of data for the projection of 2-D shape on the line of $y = -x$ and $y = x$.

As a result, we may define them via equations 4 and 5 in the following manner:

$$SD1 = (\text{Var}\ ((X(m) - Y(m))/(2)^{1/2}))^{1/2}, \quad (6)$$
$$SD2 = (\text{Var}\ ((X(m) + Y(m))/(2)^{1/2}))^{1/2}, \quad (7)$$

where Var (.) is the variance of $d1 = (X(m) - Y(m)) / (2)^{1/2}$ and $d2 = (X(m) + Y(m)) / (2)^{1/2}$ (22).

In this work, STD = π (SD1 x SD2) is used as a geometrical feature. The terms SD1 and SD2 are shown in Figure 5.

Summation of triangle area using consecutive points (*STA*)

For every three consecutive points of the shape of the Poincaré plot in 2-D space, there is only one triangle. To measure the covered area by shape in 2-D space, STA is defined, which can be formulated as follows (28, 30):

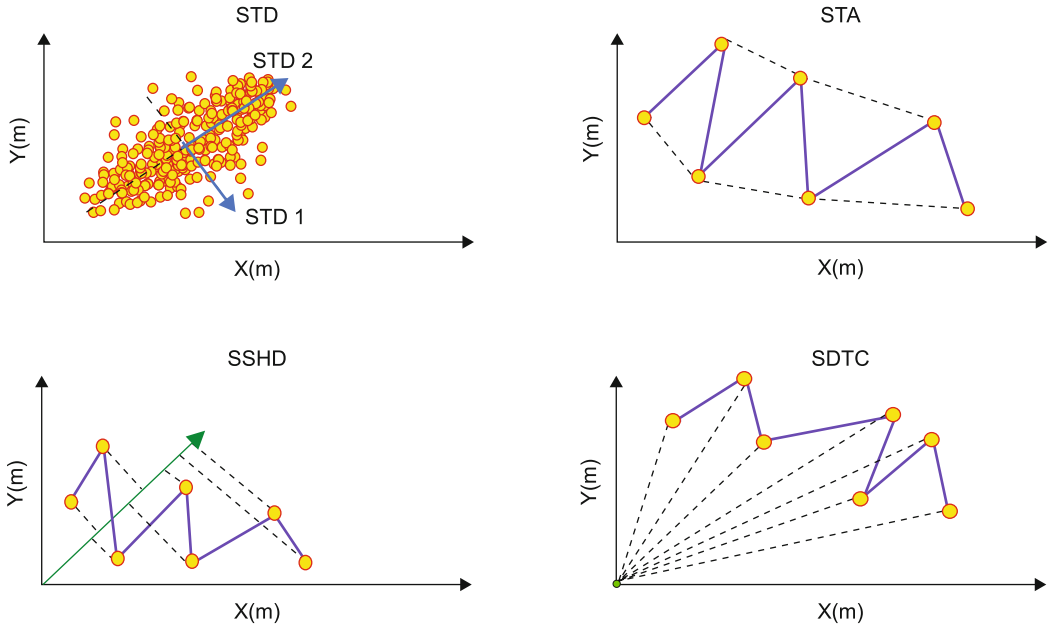

Fig. 5. Schematic illustration of STD (up-left), STA (up-right), SSHD (down-left) and SDTC (down-right) as extracted geometrical features.

$$STA = \frac{1}{2}\sum_{i=1}^{m-2}\left|\det\begin{bmatrix} X(i) & X(i+1) & X(i+2) \\ Y(i) & Y(i+1) & Y(i+2) \\ 1 & 1 & 1 \end{bmatrix}\right|, \quad (8)$$

where m is the number of Poincaré plot arrays (see Equation 3); [X (i) Y (i)], [X (i+1) Y (i+1)] and [X (i+2) Y (i+2)] indicate how to coordinate three consecutive points of Poincaré plot shape in a 2-D space. Figure 5 shows the STA as a geometrical feature.

Summation of the shortest distance from each point relative to the 45-degree line (SSHD)

In order to measure the width of shape in 2-D space, SSHD is defined which can be calculated as follows (1, 8):

$$SSHD = \sum_{i=1}^{m}\frac{|X(i)-Y(i)|}{\sqrt{2}}. \quad (9)$$

Here, [X (i) Y (i)] indicates the coordinates of each point of shape in the 2-D space. Figure 5 shows the SSHD as a geometrical feature.

Summation of distance from each point relative to a coordinate center (SDTC)

By checking the scattering of points from center of the Cartesian coordinate for 2-D shape of EEG signals in S and SF groups (See Figure 4), it is clear that Poincaré plot of coefficients of EEG signal in the S group occupies a larger area than in the SF group which can be a significant parameter for distinguishing these two groups; for this reason, here, the SDTC is used as a feature which can be formulated as follows (12, 33):

$$SDTC = \sum_{i=1}^{m}\sqrt{X(i)^2 + Y(i)^2}, \quad (10)$$

where [X (i) Y (i)] indicates the coordinates of each point of shape in the 2-D space. Figure 5 shows the SDTC as a geometrical feature.

Binary particle swarm optimization (BPSO)

Particle swarm optimization (PSO) is one of the herd-based heuristic methods which has been introduced by Eberhart and Kennedy in 1995 (44). The process of PSO consists in finding the optimal solutions based on the behavior of leaderless groups of animals commonly occurring in animal societies that reach food by random movement (45). All of them follow the member at the closest distance to the food source (global best) and others, while remembering their past position (local best), simultaneously reach their best position through communication with members with a better position (46). The group member occurring in the site with better conditions informs others who move simultaneously toward that place (i.e., towards the global solution) (47). This process is repeated until the best condition (global optimum solution) is obtained. The considered process is controlled by means of a parameter known as velocity. There are many applications and requirements of accuracy in results using several versions of PSO. Since the starting point of the original PSO is that of detecting continuous variables, and the electrode selection is a binary variable, in this paper, a binary PSO (BPSO) version is selected.

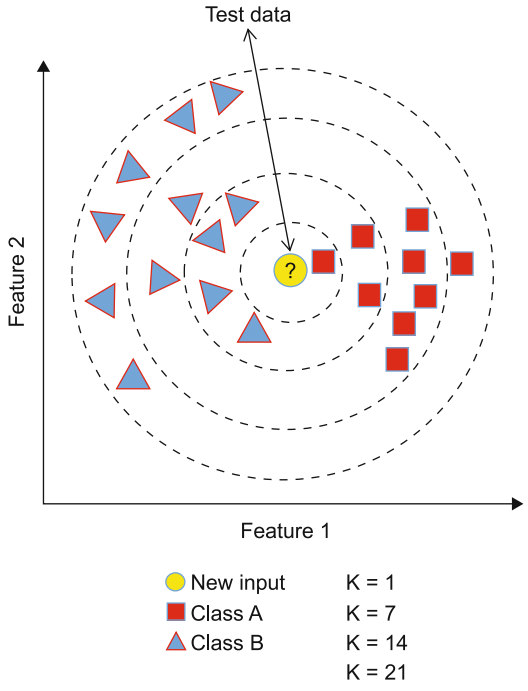

Fig. 6. KNN algorithm is illustrated as a used classifier.

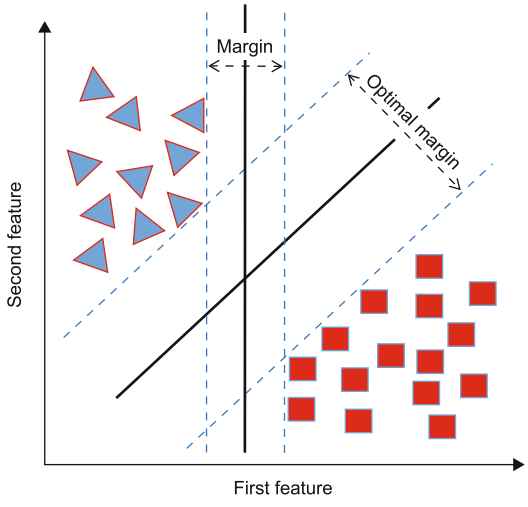

Fig. 7. The SVM algorithm is illustrated as a used classifier.

BPSO is a discrete version of PSO in a way that the process of updating a particle's velocity in BPSO is similar to PSO, yet, unlike in PSO, the particles in BPSO are comprised of either a 0 or 1 (46). The main computational steps of PSO and hence, those of BPSO, are generating the initial position and velocity of each particle in the population, and position and velocity continues to be updated until the convergence condition which characterizes the optimal solution appears.

The EEG signal has a complex structure, and its performance is considered a non-linear function (48). The PSO is one of the best choices in selecting extracted features from EEG signals because the PSO algorithm has a non-linear and stochastic nature (49). Also, it is easy to implement, and there are few parameters to adjust. In the current work, the BPSO is used as feature selection to choose the significant features. Therefore, as a result, the proposed framework becomes faster and simpler than in previous methods.

In order to implement BPSO as a features selection method in MATLAB, the written function by Jingwei Too (50) is used, in which the fitness function is set to classification performance, acceleration factors set to 2, maximum and minimum velocity set to 6, and -6, and maximum and minimum bounds on inertia weights are confined to 0.9 and 0.4. An initial population of N particles has been varied from 1 to 10.

Classifiers

In order to classify the selected features by BPSO, two well-known classifiers namely k-nearest neighbor (KNN) and support vector machine (SVM) are used.

The KNN is a simple classifier that classifies each of input data based on the nearest train data points (51, 52), for example when assuming that two features have been extracted and used as train data in a KNN classifier (Fig. 6). For classifying the test data, the KNN algorithm considers the nearest data points that are closed to the test data. In fact, the test data belong to class A (i.e., squares) when the KNN classifier checks just the first closed train data, and belongs to class B when it checks seven closed train data points and in a similar way, while the test data belong to class A and B when KNN classifier checks 14 and 21 nearest points to test the data. Thus, it is clear that the output of the KNN classifier is dependent on the number of closed train data points that the KNN classifier is considered to classify (53). In the present work, in order to choose the best value for the number of closed nearest data points, the k value varies from 1 to 9 by step 2 and the best k value is used. Another important parameter of the KNN classifier is how to calculate the distance which in the current work, it is chosen to be the Euclidean and City-block metrics.

On other hand, the SVM classifier draws a margin with the highest width between the classes in train data and then classifies the test data by considering this margin (Fig. 7) (54). In order to define the best margin, the test data points are plotted in a higher dimensional space by kernel functions (55). In the current work, the performance of SVM classifier for three different kernel functions such as linear, polynomial, and radial basis function (RBF) is tested.

Results

In the current work, DWT decomposes EEG signals into four levels. Figure 3 shows an EEG signal and its coefficients for the S ad SF groups. After that, the Poincaré plot is applied to plot the 2-D projection for DWT coefficients. It is evident that the Poincaré plot of coefficients of S EEG signals occupies a larger area than the Poincaré plot of coefficients of SF EEG signals (Fig. 4). For this reason, the Poincaré plot of coefficients was used to

Tab. 1. P-values of geometrical features for DWT sub-bands.

Window size	Feature	A_4	D_4	D_3	D_2	D_1
500	STD	8.04E-40	1.45E-42	8.37E-44	7.15E-44	5.64E-44
	STA	5.29E-41	1.24E-42	7.59E-44	8.05E-44	7.15E-44
	SSHD	8.27E-42	1.20E-42	3.73E-44	2.83E-44	3.44E-44
	SDTC	2.99E-37	1.77E-42	4.11E-44	2.88E-44	3.65E-44
1,000	STD	7.89E-40	4.70E-43	3.58E-44	4.28E-44	3.65E-44
	STA	8.12E-42	3.87E-43	3.06E-44	4.03E-44	3.80E-44
	SSHD	3.68E-42	1.60E-43	1.79E-44	1.69E-44	1.76E-44
	SDTC	2.83E-37	2.19E-43	1.94E-44	1.62E-44	1.86E-44
2,000	STD	1.32E-40	1.84E-43	3.31E-44	3.12E-44	3.31E-44
	STA	1.03E-42	1.60E-43	3.00E-44	2.72E-44	4.03E-44
	SSHD	6.30E-43	8.88E-44	1.53E-44	1.33E-44	1.62E-44
	SDTC	4.74E-38	1.17E-43	1.76E-44	1.30E-44	1.69E-44
4,000	STD	5.11E-42	1.24E-43	2.83E-44	2.88E-44	3.95E-44
	STA	2.33E-43	1.02E-43	2.61E-44	2.72E-44	3.18E-44
	SSHD	1.54E-43	6.74E-44	1.59E-44	1.11E-44	1.56E-44
	SDTC	9.88E-40	1.12E-43	1.69E-44	1.16E-44	1.59E-44

compute four geometrical features, and thus the chaotic behavior is quantified for EEG signals that consist of STD, STA, SSHD, and SDTC.

These features are directly applied to the samples. In other words, there is a direct relationship between the window sizes and the number of extracted features. Hence, the Poincaré plot of coefficients utilized to compute the proposed geometrical features for S and SF classes with various window sizes were considered for EEG signals including 500, 1,000, 2,000, and 4,000 samples.

P-value was considered to evaluate the ability of the features for discrimination between two classes (29). In this regard, the lower p-value provides a better ability for discriminating between various classes. In this work, the Kruskal-Wallis function is used for p-value computation in MATLAB software package (56).

In Table 1, p-values are written for the extracted features corresponding to DWT coefficients.

It can be seen that all geometrical features have a great ability to discriminate between S and SF EEG signals (p-value ≈ 0) within all window sizes. In other words, all of the extracted geometrical features can be fed as effective features to classifiers, but in order to decrease the value of calculation in classifiers, the size of the feature set is determined by BPSO to use just the best combination of features vector with the fewer features arrays.

In order to evaluate the performance of classifiers, the 10-fold cross-validation (CV) technique is used in which, the first step is to break the input database (i.e., Bonn university database) into ten equal subsets. Then the classifier is tested ten times with one of these sub-sets and by the nine other remaining sub-sets. As a consequence, in 10-fold CV strategy, each subset is used once as test data and nine times as train data.

The output of the classifier based on test data and its label can be categorized in four situations as described below:

True-positive (TP): when the label of test data is S and classifiers correctly classify it as S group.

True-negative (TN): when the label of test data is SF and classifiers correctly classify it as SF group.

False-positive (FP): when the label of test data is SF and classifiers incorrectly classify as S group.

False-negative (FN): when the label of test data is S and classifiers incorrectly classify it as SF group.

In each fold of the classifier, the output of a classifier is one of the latter four conditions. After training and testing the classifier ten times (i.e., the same 10-fold CV), the summation of these parameters is used to evaluate the performance of the classifier.

In this work, six different objective parameters are defined to evaluate the classification performance as follows below:

Accuracy (ACC): ability of the classifier to find a correct separation of S and SF classes. Sensitivity (SEN): ability of the classifier to find a correct classification of signals with S labels in S class.

Specificity (SPE): ability of the classifier to find a correct classification of signals with SF labels in SF class.

Positive predictive value (PPV): ability of the classifier to find a correct detection of signals with S labels between S and SF signals.

Negative predictive value (NPV): ability of the classifier to find a correct detection of signals with SF labels between S and SF signals. These parameters have been formulated as follows below:

$$ACC = \frac{TP + TN}{TP + TN + FP + FN} \text{x}100, \tag{11}$$

$$SEN = \frac{TP}{TP + FN} \text{x}100, \tag{12}$$

$$SPE = \frac{TN}{TN + FP} \text{x}100, \tag{13}$$

$$PPV = \frac{TP}{TP + FP} \text{x}100, \tag{14}$$

$$NPV = \frac{TN}{TN + FN} \text{x}100. \tag{15}$$

Figures 11, 12, 13 and 14 illustrate the performance of SVM and KNN classifiers in various situations. In Figures 11, 12, 13 and 14, BPSO was considered to obtain the significant features in window sizes of 500, 1,000, 2,000 and 4,000, respectively.

Figures 8 to 11 demonstrate that our proposed method provides ACC classification of 99 %, 99.33 %, 98.66 %, and 99 % in window sizes of 500, 1,000, 2,000, and 4,000, respectively. Table 2 shows the selected geometrical features (i.e., STD, STA, SSHD, and SDTC) from EEG coefficients (i.e., D_1, D_2, D_3, D_4 and A_4) in window sizes of 500, 1,000, 2,000, and 4,000 samples in the best

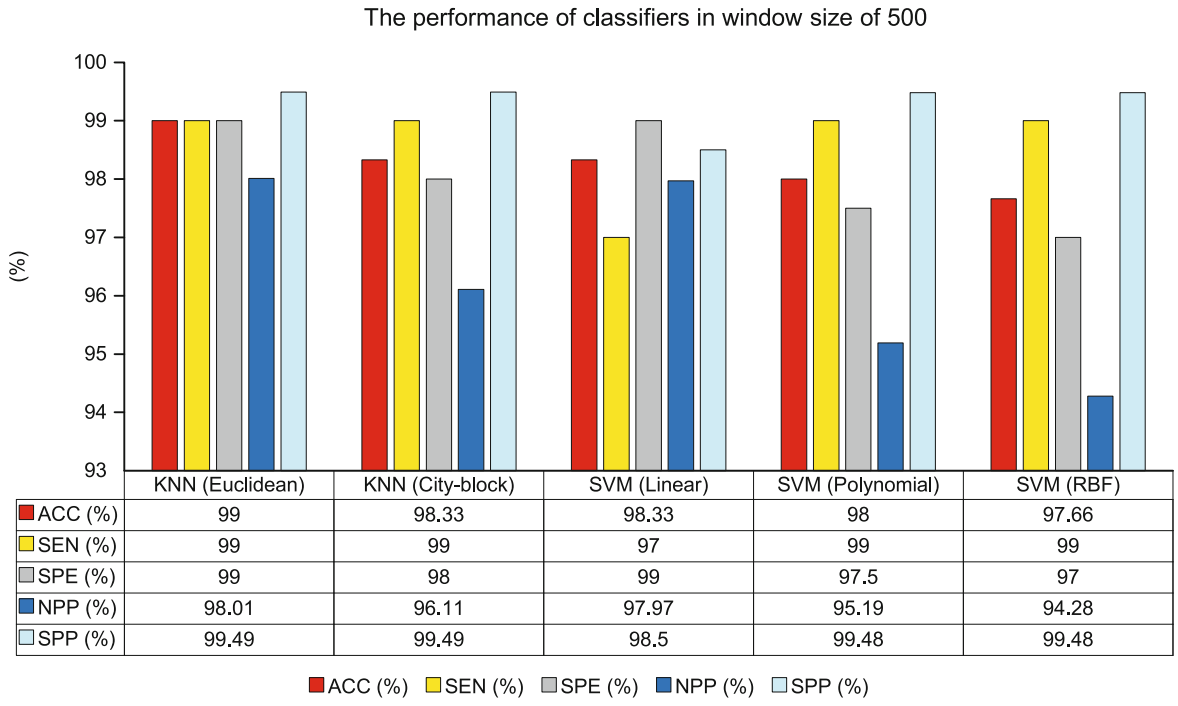

	KNN (Euclidean)	KNN (City-block)	SVM (Linear)	SVM (Polynomial)	SVM (RBF)
ACC (%)	99	98.33	98.33	98	97.66
SEN (%)	99	99	97	99	99
SPE (%)	99	98	99	97.5	97
NPP (%)	98.01	96.11	97.97	95.19	94.28
SPP (%)	99.49	99.49	98.5	99.48	99.48

Fig. 8. Comparing the performance of SVM and KNN classifiers in window size of 500.

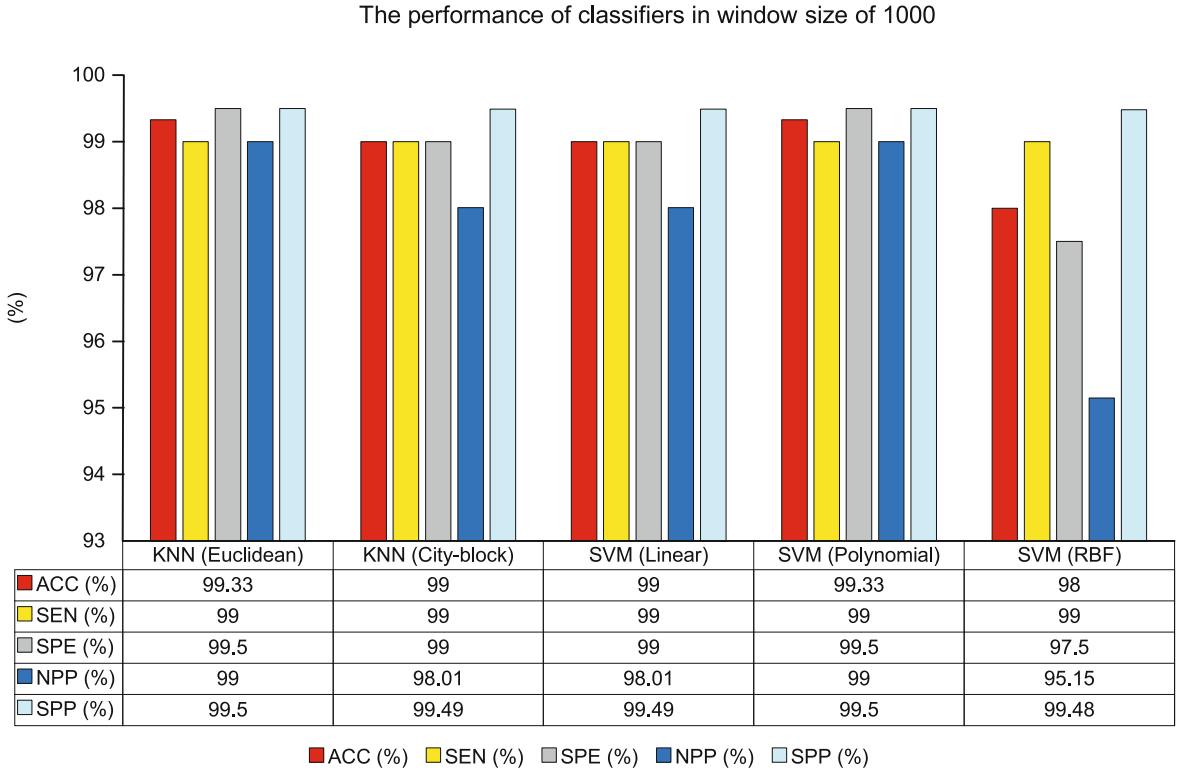

	KNN (Euclidean)	KNN (City-block)	SVM (Linear)	SVM (Polynomial)	SVM (RBF)
ACC (%)	99.33	99	99	99.33	98
SEN (%)	99	99	99	99	99
SPE (%)	99.5	99	99	99.5	97.5
NPP (%)	99	98.01	98.01	99	95.15
SPP (%)	99.5	99.49	99.49	99.5	99.48

Fig. 9. Comparing the performance of SVM and KNN classifiers in window size of 1.000.

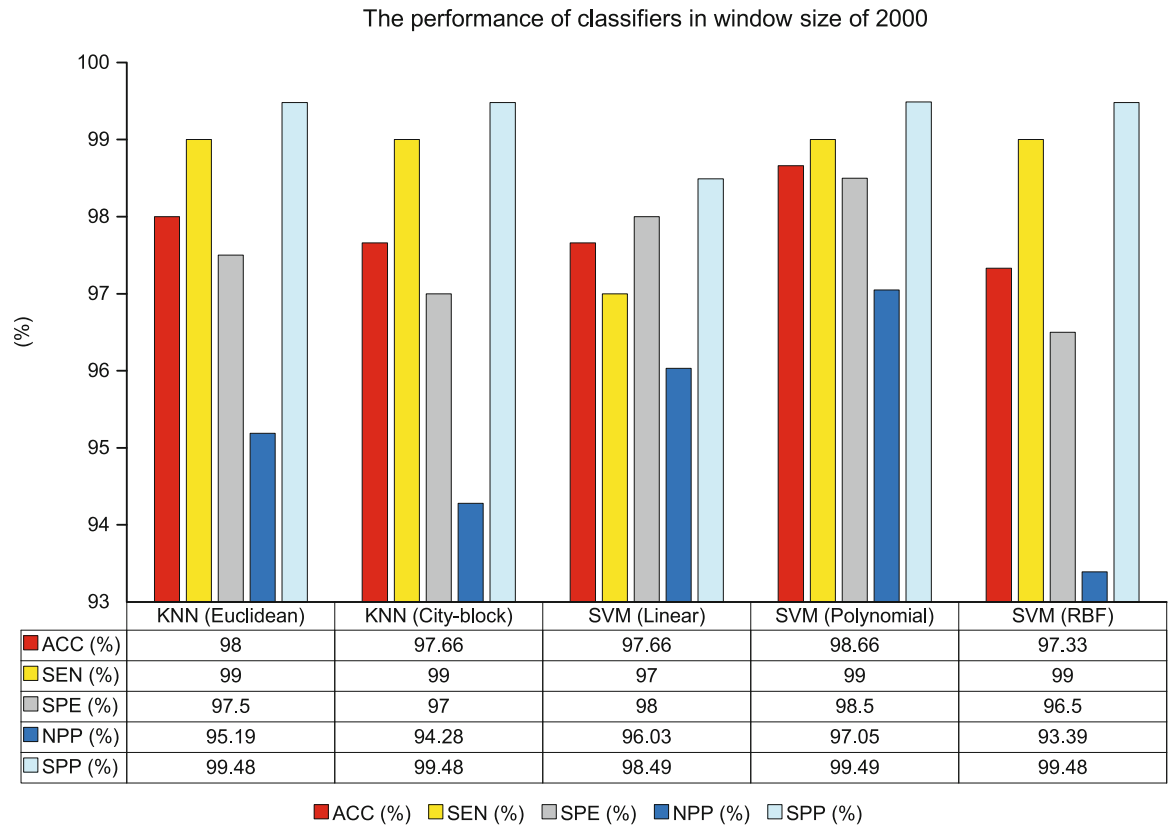

	KNN (Euclidean)	KNN (City-block)	SVM (Linear)	SVM (Polynomial)	SVM (RBF)
ACC (%)	98	97.66	97.66	98.66	97.33
SEN (%)	99	99	97	99	99
SPE (%)	97.5	97	98	98.5	96.5
NPP (%)	95.19	94.28	96.03	97.05	93.39
SPP (%)	99.48	99.48	98.49	99.49	99.48

Fig. 10. Comparing the performance of SVM and KNN classifiers in window size of 2.000

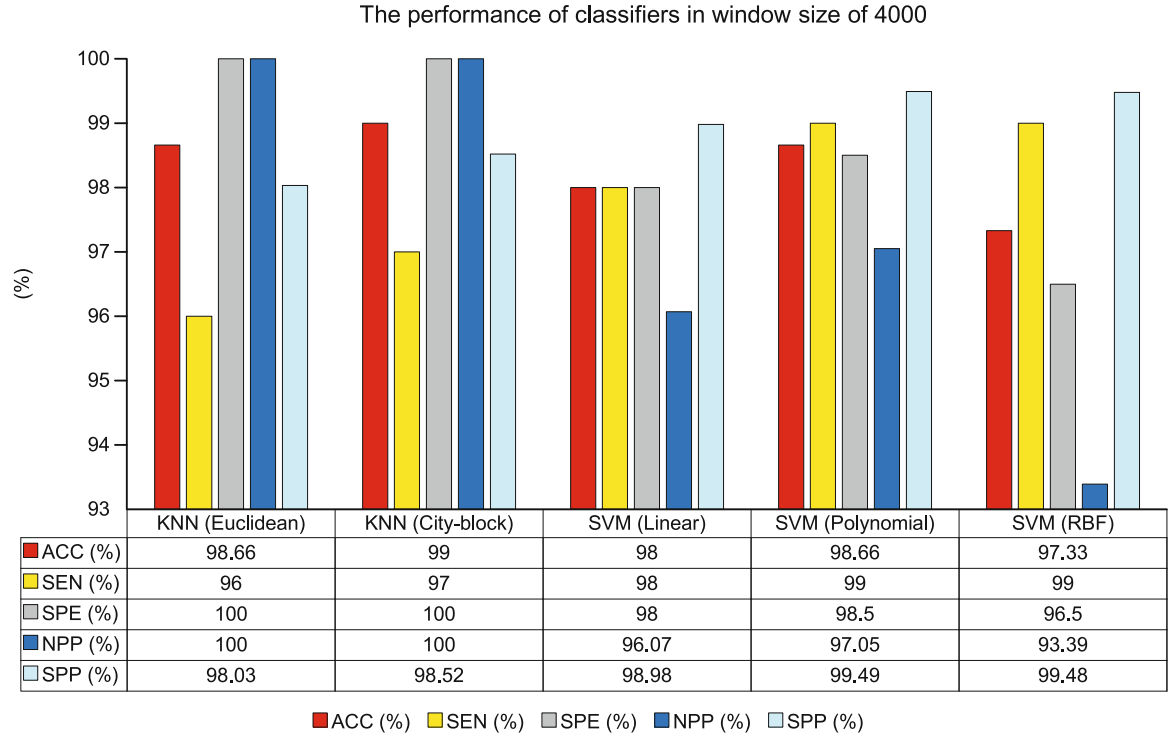

	KNN (Euclidean)	KNN (City-block)	SVM (Linear)	SVM (Polynomial)	SVM (RBF)
ACC (%)	98.66	99	98	98.66	97.33
SEN (%)	96	97	98	99	99
SPE (%)	100	100	98	98.5	96.5
NPP (%)	100	100	96.07	97.05	93.39
SPP (%)	98.03	98.52	98.98	99.49	99.48

Fig. 11. Comparing the performance of SVM and KNN classifiers in window size of 4,000.

Tab. 2. Selected geometrical features from EEG coefficients in window sizes of 500, 1,000, 2,000 and 4,000.

Window size	Classifier	STD	STA	SSHD	SDTC
500	KNN (Euclidean)	D_4, D_3	D_3, D_2, D_1	A_4, D_3, D_1	A_4, D_4, D_2
1000	KNN (Euclidean)	A_4, D_3	D_1	D_4, D_1	D_3, D_1
	SVM (Polynomial)	D_3, D_2	A_4, D_2, D_1	D_2	A_4, D_4, D_3, D_2
2000	SVM (Polynomial)	D_2, D_1	A_4, D_2, D_1	D_4, D_1	A_4, D_4, D_2
4000	KNN (City-block)	A_4, D_4, D_1	A_4, D_1	D_3	A_4, D_4, D_3, D_2

classifications, respectively. In Table 2, BPSO was used to select the geometrical features.

The algorithm run time for the proposed framework to do the preprocessing, DWT decomposition, plotting coefficients by Poincaré plot, and feeding the selected features to classifiers was 0.2 ± 0.05 seconds for the EEG signals with 4,000, 2,000, 1,000, and 500 samples. All steps of the proposed framework are implemented in MATLAB 2014a software by a system with i5-M480 CPU (2.67 GHz) and 6GB RAM. The proposed framework is fast owing to the use of few features to classify the EEG signals. Besides, the run time for the proposed framework can be faster by implementing and developing codes by C++ programming.

Discussion

We showed that the Poincaré plot of DWT coefficients of EEG signals can be employed as a usable way to decode the complexity of S and SF signals. As shown in Figure 4, the Poincaré plot for coefficients of the S EEG signals occupies more space as compared to SF EEG signals. This result has been stated in earlier studies. It has been implemented by drawing the IMFs for S and SF EEG signals in 2-D plane of SODP (24) and RPS (27). As it can be observed in the Figure 4, Poincaré plot for SF EEG signals contains more regular geometrical shapes. It may occur due to the simultaneous response of brain neurons, leading to an increase in the S-segment of EEG signals. Table 3 provides a comparison between our suggested method and the methods available in the identical database. In some studies (15–17), two classification tasks consisting of subset C vs E and subset D vs E have been assessed. On the other hand, according to some studies (18–22, 24, 25, 27), the proposed methods have been evaluated by subsets C, D vs E classification task. In study (15), permutation entropy and SVM classifier have been applied to classify S and SF EEG signals. In study (16), in order to detect S EEG signals in KNN classifier, mean degree and mean strength of HVG have been examined. According to study (17), signals, clustering technique and SVM classifier have been utilized to classify S from SF EEG. In study (18), for S and SF EEG signals classification, linear prediction error energy feature is applied to SVM classifier. In study (19), FLP error and signal energy are employed with the aim of distinguishing features between S and SF EEG signals. In study (21), several entropies and statistical features are calculated as an input to general regression neural network (GRNN) classifier. As a result, S and SF EEG signals are distinguished. In study (21), autoregressive modeling based on EMD has been represented in order to detect S. In study (22), TQWT and Kraskov entropy were used to classify S from SF EEG signals. In consonance with study (25), IEVDHM–HT was suggested to have a time-frequency representation in S and SF EEG signals. Thus, as a feature, the Rényi entropy is extracted and then applied to the least-square SVM (LS-SVM). Studies (24) and (27) report that according to the elliptical patterns of SODP and RPS IMFs in EEG signals, two-dimensional predictions have been calculated as distinguishing features between S and SF EEG signals with a 95 % confidence area. Then, they are applied to LS-SVM and artificial neural network (ANN) classifiers, respectively.

It is clearly obvious that the mentioned geometrical method resulted in the highest classification ACC as compared to the latest existing methods including references (16–22, 24, 27). Although the reported ACC classification in reference (25) is slightly higher than that in our method, their method requires heavy calculations for the associated eigenvalue decomposition and Hilbert transform computation as EEG signal processing tools. In study (25), authors clearly mentioned that: "The proposed method contributes to a good resolution in time frequency domain but calculating many components and merging them is required. Due to this reason, higher computational complexity is required in comparison with Hilbert–Huang transform method". In addition, despite the Hilbert–Huang transform, commonly known as the EMD method, it endures mode-mixing problem and noise sensitivity. Furthermore, the method mentioned by us is not sensitive to noise. Therefore, from the noise point of view, we can argue that the method proposed by us has a better performance than the method used in reference in terms of simplicity and flexibility (25).

Tab. 3. Comparison of the suggested method with the available studies in this area.

Reference number (year)	Used CV	Classification task	ACC (%)
15 (2012)	No	C vs E D vs E	88.00 79.94
16 (2014)	10-fold	C vs E D vs E	98 93
17 (2011)	10-fold	C vs E D vs E	97.69 93.91
18 (2010)	No	C, D vs E	94
19 (2014)	No	C, D vs E	95.33
20 (2016)	10-fold	C, D vs E	95.15
21 (2019)	No	C, D vs E	95.10
22 (2017)	10-fold	C, D vs E	97.5
25 (2018)	10-fold	C, D vs E	100
24 (2014)	10-fold	C, D vs E	97.75
27 (2015)	10-fold	C, D vs E	98.67
Proposed method	10-fold	C, D vs E	99.33

Conclusion

In the human brain, epileptic seizures frequently manifest spikes in EEG signals. It can visually be analyzed by experts. In long EEG records, visual inspection can be a cumbersome and time-consuming activity of detecting the presence of epileptic seizures. This paper proposes a method based on Poincaré plot of DWT coefficients for classification of S and SF EEG signals. New geometrical features are extracted from the Poincaré plot of DWT coefficients of EEG signal. The BPSO was developed to select the significant features, and then they are fed to SVM and KNN classifiers. Our proposed method has classified the S and SF EEG signals with the ACC classification of 99.33 %. Our proposed method measured the degree of complexity for Poincaré plot of DWT coefficients as a feature. It does not compute the variability of Poincaré plot, and hence it can be a good parameter for classifying EEG signals in two groups (S and SF). We also believe that geometrical features proposed by us have the ability to properly detect other disorders from EEG signals such as autism, attention-deficit hyperactivity disorder (ADHD) and Parkinson`s disease.

The empirical wavelet transform (EWT) (57) has been proposed as an adaptive tool to decompose non-stationary signals instead of the DWT method, in which the filter bank can be designed based on frequency components. Also, the sub bands of EWT have better frequency resolution than DWT. On the other hand, recently, a new time-frequency-analyzing method, namely fast iterative filtering (FIF), has been proposed to extract the modes of nonlinear and non-stationary signals (58). In fact, FIF is a fast iterative algorithm alternative to EMD, which inherits all useful properties of EMD, but has been recently proven to be convergent and not prone to mode mixing. This can lead to a method that is in some way „equivalent“ to the one proposed in study (25), but faster, reliable and stable with respect to noise. Another promising method is the adaptive local iterative filtering (ALIF) algorithm which allows to identify strong non-stationarities hidden in a signal (59). In future research, the performance of these methods will be evaluated in relation to classification of EEG signals.

References

1. Sadiq MT, Akbari H, Siuly S, Yousaf A, Rehman AU. A novel computer-aided diagnosis framework for EEG-based identification of neural diseases. Comp Biol Med 2021; 138: 104922.

2. WHO. Epilepsy, https://www.who.int/news-room/fact-sheets/detail/epilepsy, (2022).

3. Akbari H, Sadiq MT, Rehman AU. Classification of normal and depressed EEG signals based on centered correntropy of rhythms in empirical wavelet transform domain. Health Inform Sci Systems 2021; 9: 1–15.

4. Akbari H, Sadiq MT, Wen P. An Automatic Scheme with Diagnostic Index for Identification of Normal and Depression EEG Signals, Health Information Science: 10th International Conference, HIS 2021, Melbourne, VIC, Australia, October 25–28, 2021, Proceedings, Springer Nature, 2021, pp. 59.

5. Sadiq MT, Yu X, Yuan Z, Fan Z, Rehman AU, Li G, Xiao G. Motor imagery EEG signals classification based on mode amplitude and frequency components using empirical wavelet transform. IEEE Access 2019; 7: 127678–127692.

6. Sadiq MT, Yu X, Yuan Z, Zeming F, Rehman AU, Ullah I, Li G, Xiao G. Motor imagery EEG signals decoding by multivariate empirical wavelet transform-based framework for robust brain–computer interfaces. IEEE Access 2019; 7: 171431–171451.

7. Sadiq MT, Yu X, Yuan Z. Exploiting dimensionality reduction and neural network techniques for the development of expert brain-computer interfaces. Expert Systems with Applications, 164 114031.

8. Akbari H, Ghofrani S, Zakalvand P, Sadiq MT. Schizophrenia recognition based on the phase space dynamic of EEG signals and graphical features. Biomed Signal Proc Control 2021; 69: 102917.

9. Sadiq MT, Wang H. Auto-correlation Based Feature Extraction Approach for EEG Alcoholism Identification, Health Information Science: 10th International Conference, HIS 2021, Melbourne, VIC, Australia, October 25–28, 2021, Proceedings, Springer Nature, 2021, pp. 47.

10. Gupta V, Pachori RB. FBDM based time-frequency representation for sleep stages classification using EEG signals. Biomed Signal Proc Control 2021; 64: 102265.

11. HussainW, Sadiq MT, Siuly S, Rehman AU. Epileptic seizure detection using 1 D-convolutional long short-term memory neural networks. Appl Acoustics 2021; 177: 107941.

12. Akbari H, Esmaili S. A Novel Geometrical Method for Discrimination of Normal, Interictal and Ictal EEG Signals. Traitement du Signal 2020; 37: 59–68.

13. Sadiq MT, Akbari H, Rehman AU, Nishtar Z, Masood B, Ghazvini M, Too J, Hamedi N, Kaabar MK. Exploiting Feature Selection and Neural Network Techniques for Identification of Focal and Nonfocal EEG Signals in TQWT Domain. J Healthcare Engineer 2021.

14. Akbari H, Saraf Esmaili S, Farzollah Zadeh S. Detection of Seizure EEG Signals Based on Reconstructed Phase Space of Rhythms in EWT Domain and Genetic Algorithm. Signal Proc Renewable Energy 2020; 4: 23–36.

15. Nicolaou N, Georgiou J. Detection of epileptic electroencephalogram based on permutation entropy and support vector machines. Expert Systems Appl 2012; 39: 202–209.

16. Zhu G, Li Y, Wen PP. Epileptic seizure detection in EEGs signals using a fast weighted horizontal visibility algorithm. Computer Methods Programs Biomed 2014; 115: 64–75.

17. Li Y, Wen PP. Clustering technique-based least square support vector machine for EEG signal classification. Computer Methods Programs Biomed 2011; 104: 358–372.

18. Altunay S, Telatar Z, Erogul O. Epileptic EEG detection using the linear prediction error energy. Expert Systems Appl 2010; 37: 5661–5665.

19. Joshi V, Pachori RB, Vijesh A. Classification of ictal and seizure-free EEG signals using fractional linear prediction. Biomed Signal Proc Control 2014; 9: 1–5.

20. Swami P, Gandhi TK, Panigrahi BK, Tripathi M, Anand S. A novel robust diagnostic model to detect seizures in electroencephalography. Expert Systems Appl 2016; 56: 116–130.

21. Rafik D, Larbi B. Autoregressive Modeling Based Empirical Mode Decomposition (EMD) for Epileptic Seizures Detection Using EEG Signals. Traitement du Signal 2019; 36.

22. Patidar S, Panigrahi T. Detection of epileptic seizure using Kraskov entropy applied on tunable-Q wavelet transform of EEG signals. Biomed Signal Proc Control 2017; 34: 74–80.

23. Akbari H, Ghofrani S. Fast and accurate classification f and nf EEG by using sodp and EWT. Internat J Image Graph Signal Proc 2019; 11: 29–35.

24. Pachori RB, Patidar S. Epileptic seizure classification in EEG signals using second-order difference plot of intrinsic mode functions. Computer Methods Programs Biomed 2014; 113: 494–502.

25. Sharma RR, Pachori RB. Time-frequency representation using IEVDHM-HT with application to classification of epileptic EEG signals. IET Science, Measurement Technol 2017; 12: 72–82.

26. Huang NE, Shen Z, Long SR, Wu MC, Shih HH, Zheng Q, Yen NC, Tung CC, Liu HH. The empirical mode decomposition and the Hilbert spectrum for nonlinear and non-stationary time series analysis, Proceedings of the Royal Society of London. Series A: Mathematical Physical Engin Sci 1998; 454: 903–995.

27. Sharma R, Pachori RB. Classification of epileptic seizures in EEG signals based on phase space representation of intrinsic mode functions. Expert Systems Appl 2015; 42: 1106–1117.

28. Akbari H, Sadiq MT, Rehman AU, Ghazvini M, Naqvi RA, Payan M, Bagheri H, Bagheri H. Depression recognition based on the reconstruction of phase space of EEG signals and geometrical features. Appl Acoustics 2021; 179: 108078.

29. Sadiq MT, Akbari H, Siuly S, Li Y, Wen P. Alcoholic EEG signals recognition based on phase space dynamic and geometrical features. Chaos Solitons Fractals 2022; 158: 112036.

30. Akbari H, Sadiq MT, Payan M, Esmaili SS, Baghri H, Bagheri H. Depression Detection Based on Geometrical Features Extracted from SODP Shape of EEG Signals and Binary PSO. Traitement du Signal 2021; 38.

31. Goshvarpour A, Goshvarpour A. A novel 2-piece rose spiral curve model: Application in epileptic EEG classification. Computers Biol Med 2022: 105240.

32. Sadiq MT, Yu X, Yuan Z, Aziz MZ, Rehman AU, Ding W, Xiao G. Motor Imagery BCI Classification Based on Multivariate Variational Mode Decomposition. IEEE Transactions Emerg Topics Comput Intelligence 2022.

33. Yu X, Aziz MZ, Sadiq MT, Jia K, Fan Z, Xiao G. Computerized Multidomain EEG Classification System: A New Paradigm. IEEE J Biomed Health Inform 2022.

34. Khan SI, Qaisar SM, Pachori RB. Automated classification of valvular heart diseases using FBSEEWT and PSR based geometrical features. Biomed Signal Proc Control 2022; 73: 103445.

35. Salankar N, Qaisar SM, Pławiak P, Tadeusiewicz R, Hammad M. EEG based alcoholism detection by oscillatory modes decomposition second order difference plots and machine learning. Biocybernet Biomed Engineer 2022.

36. Dubey R, Kumar M, Upadhyay A, Pachori RB. Automated diagnosis of muscle diseases from EMG signals using empirical mode decomposition based method. Biomed Signal Proc Control 2022; 71: 103098.

37. Khare SK, Bajaj V, Sinha G. Adaptive tunable Q wavelet transform based emotion identification, IEEE transactions on instrumentation and measurement 2020.

38. Khare SK, Bajaj V. Constrained based tunable Q wavelet transform for efficient decomposition of EEG signals. Appl Acoustics 2020; 163: 107234.

39. Andrzejak RG, Lehnertz K, Mormann F, Rieke C, David P, Elger CE. Indications of nonlinear deterministic and finite-dimensional structures in time series of brain electrical activity: Dependence on recording region and brain state. Phys RevE 2001; 64: 061907.

40. Akbari H, Sadiq MT. Detection of focal and non-focal EEG signals using non-linear features derived from empirical wavelet transform rhythms. Phys Engineer Sci Med 1–15.

41. Khan SI, Pachori RB. Automated Detection of Posterior Myocardial Infarction From Vectorcardiogram Signals Using Fourier-Bessel Series Expansion Based Empirical Wavelet Transform. IEEE Sensors Lett 2021; 5: 1–4.

42. Goshvarpour A, Goshvarpour A. Diagnosis of epileptic EEG using a lagged Poincare plot in combination with the autocorrelation. Signal Image Video Processing 2020: 1–9.

43. Moharreri S, Dabanloo NJ, Maghooli K. Modeling the 2D space of emotions based on the poincare plot of heart rate variability signal. Biocybernet Biomed Engineeri 2018; 38: 794–809.

44. Too J, Rahim Abdullah A. Binary atom search optimisation approaches for feature selection. Connection Sci 2020: 1–25.

45. Too J, Abdullah AR, Mohd Saad N. A new quadratic binary harris hawk optimization for feature selection. Electronics 2019; 8: 1130.

46. Too J, Abdullah AR, Mohd Saad N, Tee W. EMG feature selection and classification using a Pbestguide binary particle swarm optimization. Computation 2019; 7: 12.

47. Too J, Abdullah AR, Mohd Saad N. Binary competitive swarm optimizer approaches for feature selection. Computation 2019; 7: 31.

48. Lai YC, Frei MG, Osorio I, Huang L. Characterization of synchrony with applications to epileptic brain signals. Phys Rev Lett 2007; 98: 108102.

49. Osorio I, Frei MG, Sornette D, Milton J, Lai YC. Epileptic seizures: Quakes of the brain? Phys Rev E 2010; 82: 021919.

50. Too J. Binary Particle Swarm Optimization for Feature Selection.

51. Sadiq MT, Siuly S, Rehman AU. Evaluation of power spectral and machine learning techniques for the development of subject-specific BCI, Artificial Intelligence-Based Brain-Computer Interface. Elsevier 2022, pp. 99–120.

52. Sadiq MT, Siuly S, Rehman AU, Wang H. Auto-correlation Based Feature Extraction Approach for EEG Alcoholism Identification, International Conference on Health Information Science. Springer, 2021, pp. 47–58.

53. Ghofrani S, Akbari H. Comparing nonlinear features extracted in EEMD for discriminating focal and non-focal EEG signals, Tenth International Conference on Signal Processing Systems. Internat Soc Optics Photonics 2019, pp. 1107106.

54. Sadiq MT, Yu X, Yuan Z, Aziz MZ, Siuly S, Ding W. Toward the Development of Versatile Brain– Computer Interfaces. IEEE Transactions on Artificial Intelligence 2021; 2: 314–328.

55. Yu X, Aziz MZ, Sadiq MT, Fan Z, Xiao G. A new framework for automatic detection of motor and mental imagery EEG signals for robust BCI systems. IEEE Transactions on Instrumentation Measurement 2021; 70: 1–12.

56. Sadiq MT, Yu X, Yuan Z, Aziz MZ. Motor imagery BCI classification based on novel two-dimensional modelling in empirical wavelet transform. Electronics Lett 2020; 56: 1367–1369.

57. Gilles J. Empirical wavelet transform. IEEE Transactions on Signal Processing 2013; 61: 3999–4010.

58. Cicone A, Zhou H. Numerical analysis for iterative filtering with new efficient implementations based on FFT. Numerische Mathematik 2021; 147: 1–28.

59. Cicone A, Garoni C, Serra-Capizzano S. Spectral and convergence analysis of the Discrete ALIF method. Linear Algebra Appl 2019; 580: 62–95.

Received July 8, 2022.
Accepted August 24, 2022.